Journal of Coastal Research	SI	63	68–83	Coconut Creek, Florida	Spring 2013

An Examination of Historical Inorganic Sedimentation and Organic Matter Accumulation in Several Marsh Types within the Mobile Bay and Mobile–Tensaw River Delta Region

Christopher G. Smith, Lisa E. Osterman, and Richard Z. Poore

U.S. Geological Survey
St. Petersburg Coastal and Marine Science Center
600 4th Street South
St. Petersburg, FL 33701, U.S.A.
cgsmith@usgs.gov

www.cerf-jcr.org

www.JCRonline.org

ABSTRACT

Smith, C.G.; Osterman, L.E., and Poore, R.Z., 2013. An examination of historical inorganic sedimentation and organic matter accumulation in several marsh types within the Mobile Bay and Mobile–Tensaw River delta region. *In:* Brock, J.C.; Barras, J.A., and Williams, S.J. (eds.), *Understanding and Predicting Change in the Coastal Ecosystems of the Northern Gulf of Mexico,* Journal of Coastal Research, Special Issue No. 63, pp. 68–83, Coconut Creek (Florida), ISSN 0749-0208.

Mass accumulation rates (MAR; g cm^{-2} y^{-1}), linear sedimentation rates (LSR; cm y^{-1}), and core geochronology derived from excess lead-210 (^{210}Pb) profiles and inventories measured in six sediment cores collected from marsh sites from the Mobile–Tensaw River Delta and Mobile Bay region record the importance of both continuous and event-driven inorganic sedimentation over the last 120 years. MAR in freshwater marshes varied considerably between sites and through time (0.24 and 1.31 g cm^{-2} y^{-1}). The highest MARs occurred in the 1950s and 1960s and correspond to record discharge events along the Mobile and Tensaw Rivers. In comparison, MAR at salt marsh sites increased almost threefold over the last 120 years (0.05 to 0.18 g cm^{-2} y^{-1} or 0.23 to 0.48 cm y^{-1}). From 1880 to 1960, organic accumulation remained fairly constant (~20%), while intermittent pulses of high inorganic sedimentation were observed following 1960. The pulses in inorganic sedimentation coincide with several major hurricanes (*e.g.*, Hurricanes Camille, Fredric, Georges, and Ivan). The nearly threefold increase in MAR in salt marshes during the last 120 years would thus appear to be partially dependent on inorganic sedimentation from storm events. This study shows that while hurricanes, floods, and other natural hazards are well-known threats to human infrastructure and coastal ecosystems, these events also transport sediment to marshes that help abate other pressures such as sea-level rise (SLR) and subsidence.

ADDITIONAL INDEX WORDS: *Lead-210 geochronology, mass accumulation rates, hurricanes, floods.*

INTRODUCTION

Coastal wetlands (marshes and forests) accrete through the accumulation of organic and inorganic materials (Childers and Day, 1990; Morris *et al.*, 2002; Redfield, 1972). The accumulation of these materials abates pressures associated with global climate change, eustatic (~1.8 ± 0.5 mm y^{-1}; IPCC, 2007) and relative sea-level rise, and human perturbations, all of which threaten the function and longevity of coastal wetlands (Kolker *et al.*, 2009; Moorhead and Brinson, 1995; Morris *et al.*, 2002; Patrick and DeLaune, 1990). Generalizations about reliance of certain marsh types (*i.e.*, freshwater versus brackish, interior versus fringing, tidal versus nontidal) on either inorganic sedimentation or organic accumulation are often restricted to local case studies (*e.g.*, Flessa, Constantine, and Cushman, 1977; Harrison and Bloom, 1977; Reed, 1990). Generalizing beyond the local scale is complicated by complex variables such as inundation frequency and duration, flood depth, inorganic sediment availability, and nutrient regime, among others (Reed, 1988). Recent coupled geomorphic and ecological models have begun to approximate these complex systems to better understand the feedbacks between ecology and physical environment (Kirwan and Murray, 2007, 2008; Morris *et al.*, 2002).

Like all coastal systems, coastal marshes provide a dynamic interface between the terrestrial and marine realms. Understanding modern processes (sedimentologic, hydrologic, and geochemical) at this interface provides critical information about how the terrestrial-marine continuum is responding to natural and anthropogenic perturbations. While historically (hundreds to thousands of years), marsh and forested wetlands have lost out to human development of the coast, their services have become better understood over the last 30–40 years. The most well recognized and desired function and service currently are mitigation against sea-level rise and storm impacts (IPCC, 2007). The effects of sea-level rise and storm impacts are most pronounced in areas where local and regional land subsidence exacerbate global sea-level rise. For example, the northern Gulf of Mexico coastal zones experience rates of sea-level rise that range from 2.2 to 11 mm y^{-1} (Otvos, 2004) with the highest rates occurring in coastal Louisiana. Compounding the Louisiana sea-level subsidence problem is anthropogenic modifications (*e.g.*, lock and dam construction and leveeing) to the Mississippi River system (Blum and Roberts, 2009) that have left the coastal marshes sediment starved. In other areas of the Gulf of Mexico, like Mississippi Sound and Mobile Bay, subsidence is less influential and relative rates of sea-level rise are more consistent with eustatic rates. Hence, understanding the marsh response to modern and historical global or eustatic sea-level rise is more

DOI: 10.2112/SI63-007.1 received 25 October 2011; accepted 4 June 2012.
© Coastal Education & Research Foundation 2013

applicable in these areas. In addition, the roles of inorganic sedimentation versus organic accumulation are largely unknown in this region.

In this study, we quantify accretion rates for several marsh types around the Mobile Bay and the bayhead delta. We provide the first detailed investigation on what contribution inorganic and organic materials provide to the net accretion of marshes in this region. The objective is to determine if there are coherent responses of different marsh types to documented natural processes (sea-level rise, hurricanes) or anthropogenic modifications (development, lock and dam construction), or both, within the watershed and bay.

To qualitatively distinguish between the inorganic and organic contributions to vertical marsh accretion, we use the phrases *inorganic sedimentation* and o*rganic matter accumulation*. However, in the case where quantitative rates are presented, *linear sedimentation rates* are exclusively net accretion rates in velocity units [L T^{-1}] and mass accumulation rates are mass flux rates [M L^{-2} T^{-1}]. Quantitatively, the latter can be broken down into organic matter accumulation rates [M_{org} L^{-2} T^{-1}] and mineral deposition rates [M_{inorg} L^{-2} T^{-1}].

METHODS

Site Description

Mobile Bay, located in southeastern Alabama (U.S.A.), is the drowned remnants of the Pleistocene Mobile River system (Figure 1). Following the onset of the Holocene transgression, flooding and backfilling of incised river valleys formed the bay (Kindinger, Balson, and Flocks, 1994; Mars, Shultz, and Schroeder, 1992). By approximately 8,000 cal yr B.P., the modern bay dimensions (*i.e.*, 50-km long, 39-km wide, and 3-m deep), which include part of Bon Secour Bay, were roughly present (Rodriguez *et al.*, 2008). Decreasing rates of sea-level rise between 6,000 and 8,000 cal yr B.P. allowed sediment to accumulate at the upper reaches of the bay forming a deltaic plain (Mars, Shultz, and Schroeder, 1992; May, 1976; Rodriguez *et al.*, 2008). At the same time, progradation and expansion of Morgan Peninsula occurred (Mars, Shultz, and Schroeder, 1992; Otvos, 2004; Rodriguez and Meyer, 2006) further isolating the bay from the Gulf of Mexico.

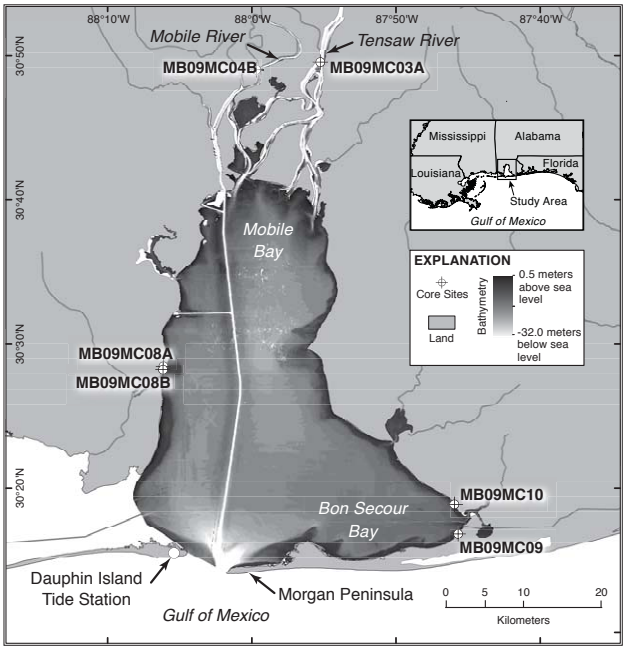

Figure 1. Map showing the regional extent of Mobile Bay and the bayhead delta and the location of the marsh cores collected, processed, and analyzed in this study.

The modern bay and bayhead delta annually receives 4.5 Tg of suspended sediment and 56.8 km^3 of water from the 107,000 km^2 drainage basin (Curtis, Culbertson, and Chase, 1973). The Alabama and Tombigbee Rivers are the main stems for the drainage basin before briefly merging into the Mobile River and then diverging into the lower distributary Mobile–Tensaw River system. The drainage basin is the fourth largest and sediment yields are the fifth largest of rivers discharging to the ocean within the conterminous United States (including the Columbia River) (Curtis, Culbertson, and Chase, 1973). Sedimentation at the head of the bay has formed the largest inland delta in the U.S. (*i.e.*, Mobile–Tensaw River Delta or MTRD) with a total area of 756 km^2. The MTRD is comprised of nontidal to tidal, freshwater bottomland hardwood forests, cypress and tupelo forests, and marsh wetlands, while the perimeter of Mobile Bay is dominated by smaller, fringing brackish to salt marsh environments.

Data for this study are based on six cores collected from three different marsh types: freshwater (MB09MC04B, MB09MC03A), interior brackish (MB09MC08A, MB09MC09), and fringing or shoreline brackish (MB09MC08B, MB09MC10; Figure 1). From this point forward in the text, the MB09 has been dropped from the core name except in the tables and figures. The freshwater marshes are located along the tidal reaches of the Mobile and Tensaw Rivers; however, we are uncertain of the extent of tidal flooding to these sites. Cores were collected between 100–200 m from the main riverbank. Vegetation diversity in the two freshwater marshes was slightly different but *Typha* spp. dominated both sites. Interior brackish marsh sites were monospecific stands of *Juncus romerianus* and cores were collected approximately 200 m inland of the bay. Both fringing marsh sites were dominated by the *Spartina alterniflora* (tall-form). Cores were collected approximately 1 m from the shoreline adjacent to the bay.

Sediment Collection and Analysis

Each marsh core was collected using 5.2-cm diameter transparent acrylic tube. Core lengths varied from 48 to 68 cm and compaction was less than 10 cm in all cores (Table 1). Cores were sectioned in the field at 1-cm intervals for the upper 10 cm and at 2 cm for the remainder of the core. Major lithologic changes were noted in the field during sectioning and descriptive lithologies were obtained during laboratory preparation. Samples were stored refrigerated until further processing. In the laboratory, entire sediment samples were packed into a graduated syringe to acquire total volume, weighed, freeze-dried, and reweighed. Sediment bulk density (ρ_b) was calculated as the

ratio of the measured dry sediment mass (M_t, g) to the measured total volume (V_t, cm^3). Porosity (φ) was estimated using

$$\varphi = \left(\frac{M_t - M_d}{\rho_w} \right) \Big/ V_t \tag{1}$$

where M_d is the dry sediment mass (g) and ρ_w is water density (g cm^{-3}) (Breitzke, 2006). Water density was estimated using a linear approximation ($\rho_w = 1+0.0008S$) as a function of pore-water salinity (S) (Breitzke, 2006). Bulk organic matter (OM) content was measured on 5 g of sediment using mass loss-on-ignition (LOI) at 550˚C (Oertel, Wong, and Conway, 1989). Average relative standard deviation (RSD) for 25% replication of all samples was ~4%.

Approximately 20 g of each dried core section was homogenized with a mortar and pestle, packed into an airtight cup, and aged for approximately 30 days. Total lead-210 (^{210}Pb), radium-226 (^{226}Ra), and cesium-137 (^{137}Cs) were measured using a planar-style high-purity, low-energy, germanium gamma-ray spectrometer (Canberra, Inc). Total ^{210}Pb and ^{137}Cs were determined using photopeaks 46.5 and 661.6 keV, respectively. Supported ^{210}Pb (sediment-bound ^{226}Ra) was estimated using the 295.1 and 352.1 keV photopeaks for ^{214}Pb and the 609.3 keV photopeak for bismuth-214 (^{214}Bi) (Cutshall, Larsen, and Olsen, 1983; Robbins and Edgington, 1975). All samples were corrected for self-absorption using a ^{238}U sealed-source following the procedure outlined by Cutshall, Larsen, and Olsen (1983). Counting efficiencies for U-series radionuclides were determined using IAEA-RGU-1 standard. Efficiency for ^{137}Cs was interpolated by counting efficiencies for peaks between 295 and 1239 keV.

Radionuclide Inventories, Mass Accumulation Rates, and Geochronologic Models

Inventories of ^{210}Pb$_{xs}$ and ^{137}Cs provide information concerning the depositional record preserved in the sediments and help assess assumptions implied by common geochronologic models. Given the irregularity in the sample intervals, mass depth was estimated using the trapezoid rule

$$m_n = m_{n-1} + 0.5\left(\rho_{b_n} + \rho_{b_{n-1}}\right)\left(z_n + z_{n-1}\right) \tag{2}$$

where, m_n is mass depth (g cm^{-2}), z_n is the depth (cm), and ρ_{b_n} is bulk density (g cm^{-3}) for sample n. Cumulative inventories ($^{+}I_{m_n}$; dpm cm^{-2}) above mass depth (m_n) for each radionuclide was computed using specific activity (A_{m_n}; dpm g^{-1}) and mass depth

$$^{+}I_{m_n} = {}^{+}I_{m_{n-1}} + 0.5\left(A_{m_n} - A_{m_{n-1}}\right)\left(m_n - m_{n-1}\right) \tag{3}$$

Mass accumulation rates (MAR), linear sedimentation rates (LSR), and chronology were assessed using a combination of ^{210}Pb and ^{137}Cs data. Long-term trends in the mass accumulation were assessed using a simple advection-decay model (Appleby, 2001; Appleby and Oldfield, 1978; Robbins and Edgington, 1975), which assumes constant mass accumulation and ^{210}Pb flux to the marsh surface

$$A_{m_n} = A_0 e^{-\lambda m_n/\omega} \tag{4a}$$

where λ is the decay constant (0.03108 y^{-1}) and ω is MAR (g cm^{-2} y^{-1}). Transforming 4a by taking the natural logarithm of

Table 1. *A summary of depth-integrated ^{210}Pb and ^{137}Cs inventories and related parameters obtained for various marsh cores from Mobile Bay and bayhead delta region. For comparison, inventories are provided for the Gulf of Mexico region, the southeastern United States of America, and similar latitudinal extents.*

Core ID	Core Length (cm)	Mixing Zone (cm)	Surface Actvity (dpm g^{-1})	^{210}Pb Inventory (dpm cm^{-2})	Invent. Err (dpm cm^{-2})	Depth Observed (cm)	^{137}Cs Inventory (dpm cm^{-2})	Invent. Err (dpm cm^{-2})
MB09MC04B	62	n/a	4.13	36.23	5.69	46	3.26	0.29
MB09MC03A	54	n/a	2.56	32.30	3.43	44	8.11	0.85
MB09MC08A	42	n/a	4.70	23.29	3.34	28	7.15	0.24
MB09MC09	36	12	1.90	34.09	7.39	36	7.34	0.38
MB09MC08B	62	n/a	4.23	73.42	7.09	42	0.82	0.17
MB09MC10	45	n/a	0.90	26.73	2.39	31	10.08	0.45
Average			3.07	37.68	18.20		6.13	3.42
Q1				28.12	-		4.23	-
Q3				35.70	-		7.92	-
Q3-Q1				7.57	-		3.68	-
Average (3*(Q1-Q3) outliers)				30.53	5.37			-
Southern North America (Appleby and Oldfield, 1992)				29.70	12.80		-	-
Continental 30º to 40ºN (Preiss, Mélières, and Pourchet, 1996)				31.87				
Global 30º to 40ºN Latitude (Baskaran, 2011)				30.89	18.70		-	-
Ideal Coastal Louisiana (Milan *et al.*, 1995)				-	-		5.29	-
Average Coastal Louisiana (Milan *et al.*, 1995)				-	-		5.88	2.60

both sides forms a linear relationship between activity and mass depth

$$\ln\left(A_{m_n}\right) = \ln\left(A_0\right) - \lambda m_n / \omega \quad (4b)$$

where the slope (S) of the line is λ/ω. A similar approach can be used for LSR (r; cm y^{-1}) by substituting depth (z; cm) for mass depth (m_n); the slope is then equal to λ/r. Slopes were estimated using a linear regression algorithm in Sigmaplot (Systat Software, Inc.). Uncertainties in the MAR (σ_ω) and LSR (σ_r) were propagated from relative uncertainty for the slope (σ_s/S) from the regression analysis

$$\sigma_\omega = (\sigma_s/S)\omega \quad (5a)$$

$$\sigma_r = (\sigma_s/S)r \quad (5b)$$

Refined estimates and temporal variations of MARs and LSRs were determined using a variant of the advection-decay equation known as the CRS (constant rate of supply) model (Appleby and Oldfield, 1978; Binford, 1990). The CRS model assumes a constant flux of ^{210}Pb to the marsh surface irrespective of the sedimentation rate, forcing an inverse relationship between mass accumulation rate $\omega(t)$ and ^{210}Pb concentrations deposited $C(t)$

$$F_{^{210}Pb} = C(t)\omega(t) = C_{m_n}\omega_{m_n} = \text{const} \quad (6).$$

The common form of the CRS model as derived by Appleby and Oldfield (1978) is

$$^{-}I_{m_n} = {}^{+}I_0 - {}^{+}I_{m_n} = I_0 e^{-\lambda t} \quad (7a)$$

where $^{-}I_{m_n}$ is the inventory below mass depth (m_n). Rearranging the equation to solve for t_{m_n} (y) provides a direct age for each mass depth

$$t_{m_n} = \frac{1}{\lambda}\ln\left(\frac{I_0}{^{-}\mathrm{I}_{m_n}}\right) \quad 7b);$$

additional substitution and algebraic adjustments provide MAR for individual mass depths

$$\omega_{m_n} = \lambda \ln\left(\frac{^{-}\mathrm{I}_{m_n}}{C_{m_n}}\right) \quad (7c).$$

LSR can be handled in a similar fashion as that of equation 7c. Errors for age and MAR were propagated from counting errors as described by Binford (1990). The overall contribution of OM accumulation and mineral deposition can be assessed through time by applying a simple conversion to the MAR based on fraction of organic matter (f_{OM}) measured by LOI, such that the organic matter accumulation rate (orgMAR or ω_{OM}) and mineral deposition rate (MDR or ω_{MD}) are, respectively,

$$\omega_{OM} = f_{OM} \cdot \omega \quad (8a)$$

$$\omega_{MD} = \left(1 - f_{OM}\right) \cdot \omega \quad (8b)$$

RESULTS

Sediment Characteristics

Vertical profiles of percent OM (LOI-based), dry bulk density, and porosity for the six marsh cores are presented in Figure 2. The freshwater marsh sediment (cores MC03A and MC04B) demonstrates a generally fining upward pattern accented by increasing OM (from 5 to 15%) and porosity (from 0.35 to 0.55) and decreasing bulk density (from 1.25 to 0.25 g cm^{-3}). This trend in the upper portion of MC04B is interrupted at least twice with lower OM, lower porosity, and higher bulk density sediments than vertically adjacent samples. For interior brackish marsh cores (MC08A and MC09), bulk density, OM, and porosity profiles are nearly vertical. Relative to other cores, MC09 has low organic matter content (~5%) throughout most of the core; however, organic content increases by 20%, 50–65 cm below land surface (cmbls). While MC08A has much higher OM and porosity and lower bulk density than MC09, intervals of low OM and porosity and high bulk density are apparent in the profiles (*e.g.*, 4, 10, 34 cmbls; Figure 2). Fringing brackish marshes (MC08B and MC10) also show a fining upward trend; however, the overall gradients in OM, porosity, and bulk density are less than the freshwater marshes. Of all the cores, MC10 has the most distinct lithologic boundaries. The sediment exhibits two fining upward sequences (0–15 and 25–50 cmbls) separated by a relatively thick (10+ cm) medium sand layer. The sediment below the sand layer resembles the dense organic-rich sediment observed in MC08A and at the base of MC09.

Profiles and Inventories of ^{210}Pb and ^{137}Cs

Profiles of $^{210}Pb_{xs}$ and ^{137}Cs for each of the marsh cores are also presented in Figure 2. The ^{210}Pb profiles demonstrate an expected surface flux (*i.e.,* atmospheric or tidal sediment contribution) decreasing exponentially with depth. While all of the marsh cores contain quantifiable ^{137}Cs, the overall preservation of the typical step (dirac delta) function representative of the 1950 and 1960 test period is not well defined. MC08A and MC10 are the exceptions. MC08A has a well-preserved ^{137}Cs profile with a well-refined maximum (3.35 dpm g^{-1}) at 15±1 cmbls. In comparison, the ^{137}Cs maximum (1.41 dpm g^{-1}) in MC10 extends over 6 cm (20–26 cmbls) and occurs just below a sharp lithologic boundary between the organic-rich and organic-poor sediment. This raises the concern that a portion of the ^{137}Cs flux may have been lost or modified during the emplacement of the sand layer. While the overall magnitude of the two maxima differs by a factor of 2.3, the depth integrated activity for MC08A (4.1 dpm cm^{-2}) is quite similar to that observed in MC10 (4.89 dpm cm^{-2}), suggesting a similar source term for the two intervals. The difference in the thickness of the two maxima is best explained by a difference in sedimentation rate and/or source, which is supported by the physical characteristics of the sediments. However, bioturbation and reworking cannot be ruled out.

The ^{210}Pb inventories for the six marsh cores range between 23.3–73.4 dpm cm^{-2} with an average of 37.8±18.2 dpm cm^{-2} (n=6; Table 1). Variance in the data is largely due to MC08B, which has the highest inventory (73.4 dpm cm^{-2}). Excluding the

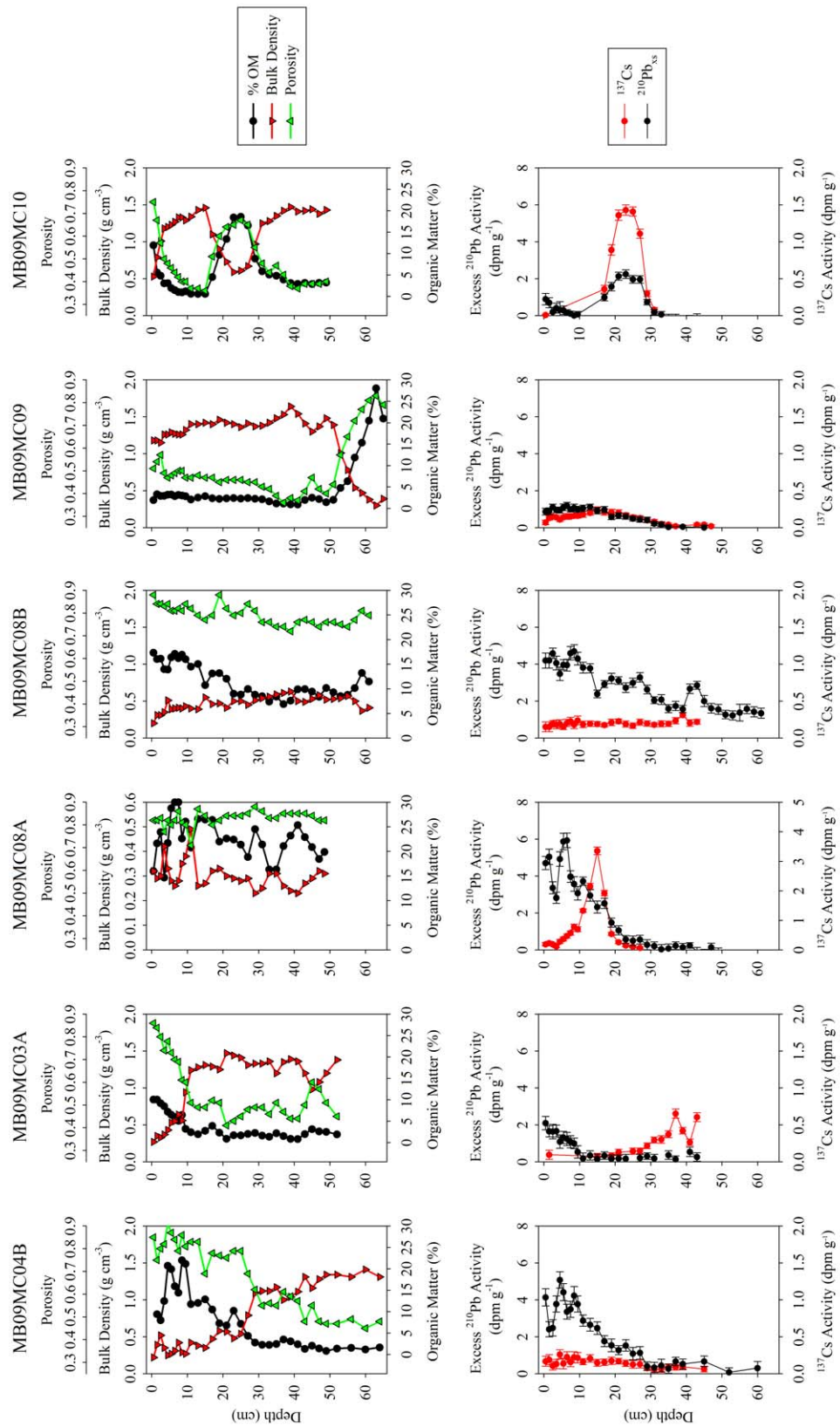

Figure 2. (Top Row) Vertical profiles of bulk density, porosity, and organic matter (percentage of loss-on-ignition) measured as well as (Bottom Row) excess lead-210 ($^{210}Pb_{xs}$) and cesium-137 (^{137}Cs) measured for the freshwater (MB09MC04B and MB09MC03A), interior brackish (MB09MC08A and MB09MC09), and fringing brackish marshes (MB09MC08B and MB09MC10). Vertical scale is presented as linear distance (cm).

Table 2. *Linear sedimentation rates and mass accumulation rates obtained for each marsh core using the constant flux-constant supply model (CF:CS) and the constant rate of supply model (CRS).*

	CF:CS		CRS		CF:CS		CRS	
Core ID	Linear Sedimentation Rate (cm y^{-1})	LSR Err	Avg. Linear Sedimentation Rate (cm y^{-1})	LSR 2s (±cm y^{-1})	Mass Accumulation Rate (g cm^{-2} y^{-1})	MAR Err (±g cm^{-2} y^{-1})	Avg. Mass Accumulation Rate (g cm^{-2} y^{-1})	MAR 2s (±g cm^{-2} y^{-1})
MB09MC04B	0.518	0.043	0.755	0.376	0.457	0.054	0.336	0.328
MB09MC03A	0.797	0.143	1.058	0.503	1.210	0.270	0.838	1.121
MB09MC08A	0.290	0.022	0.330	0.183	0.086	0.007	0.095	0.110
MB09MC09	0.706	0.100	0.592	0.494	0.972	0.121	0.575	0.660
MB09MC08B	1.480	0.141	1.153	0.925	0.758	0.055	0.370	0.320
MB09MC10	0.085	0.016	N.D.		0.08	0.009	N.D.	
Average	0.646		0.778		0.594		0.443	
SD	0.486		0.337		0.467		0.279	
Freshwater Interior Marshes	0.657	0.197	0.907	0.214	0.834	0.532	0.587	0.355
Brackish Interior Marshes	0.498	0.294	0.461	0.185	0.529	0.626	0.335	0.339

upper extreme from the mean (30.5±5.4 dpm cm^{-2}; n=5) reduces the relative standard deviation from 48% to 3%. The average $^{210}Pb_{xs}$ inventories from Mobile Bay marsh cores compare favorably with published regional (eastern North America) inventories associated with solely atmospheric inputs (29.7±12.8 dpm cm^{-2}; Appleby and Oldfield, 1978). Based on the average $^{210}Pb_{xs}$ inventory, the annual flux of ^{210}Pb from the decay of ^{222}Rn in the atmosphere to the Mobile Bay region is on the order of 0.94 dpm cm^{-2} y^{-1}.

The ^{137}Cs inventories preserved in the marsh cores range between 0.82–10.08 dpm cm^{-2} with no distinct association to marsh type (Table 1). Compared with the $^{210}Pb_{xs}$ inventories (excluding the extreme outlier, RSD=3%) the ^{137}Cs have a broader relative range (RSD=34%). The average ^{137}Cs inventory for the Mobile Bay marsh cores (6.13±3.42 dpm cm^{-2}) is slightly higher than the ideal inventory (5.29 dpm cm^{-2}) for the Gulf of Mexico but falls within the upper half of the ^{137}Cs inventories observed in Louisiana marshes (Milan *et al.*, 1995).

Mass Accumulation Rates and Geochronology

Summaries of the linear regression analyses performed for each marsh core are presented in Figures 3 and 4; summaries of MARs and LSRs are given in Table 2. The average MAR and LSR for all cores are 0.594±0.467 g cm^{-2} y^{-1} and 0.646±0.486 cm y^{-1}, respectively. Overall there are no distinct patterns among the various marsh types. For example, MAR for the two interior brackish marsh sites differ by an order of magnitude, as do the MARs for the two fringing brackish marsh sites. Intracomparison of LSR for the different marsh types is not as variable as the MAR, reflecting significant difference in the sediment composition of the accreting marsh. Examination of the regression coefficients for each of the plots suggests that simple log-linear approximation (*i.e.*, $r^2 < 0.75$) does not fully explain the depositional history of all the marsh sites.

The ^{210}Pb geochronologies provided by the CRS models suggest that for most cores, the sedimentary record extends back to the late 19th or early 20th century. The ^{137}Cs profiles support this temporal framework. For the most of the cores, the ^{137}Cs profiles were fairly uniform (Figure 5); however, the ^{210}Pb ages for the first occurrence of ^{137}Cs occurs between 1930 and 1940, a common observation for Gulf of Mexico marshes (Milan *et al.*, 1995). Based on the ^{210}Pb-derived ages, the ^{137}Cs peak in MC08A (Figure 5) was deposited between 1958–1966, bracketing well the peak in atmospheric testing (*circa* 1963). Reworking and/or diluting of mid-20th century atmospheric testing peak best explains the dampened signal in the remainder of the cores. As shown with the inventories, a majority of the cores have a ^{137}Cs record comparable to expected atmospheric flux during the 1950s and 1960s testing period.

Refined LSRs and MARs derived from the CRS model are presented in Figure 5 with a summary of the long-term averages found in Table 2. Average LSRs and MARs obtained from the CRS for each marsh site are within error of the CF:CS modeled rates (Table 2). Overall, LSRs and MARs at all the marsh locations appear to have accelerated during the last 20 years (increase of 20–80%), with the most dramatic change occurring in the brackish marshes (Figure 5). The global LSR averages for the interior freshwater marshes (MC04B and MC03A) are two times the rates observed in the interior brackish marshes (MC09 and MC08A). By the turn of the 21st century, the two marsh types accreted at a similar linear rate. Mass accumulation

in the freshwater marshes (Coefficient of Variation, CV=0.3) do not vary through time as significantly as in the brackish marshes (CV=0.6).

With the exception of MC08A, the fraction of organic matter in bulk sediment is generally low (< 15%), suggesting mineral-dominated marsh environments. Based on the temporal framework of the various cores, it would appear that the marshes have (*e.g.*, MC08B, 04B, MC03A) or are (*e.g.*, MC09, MC10) transitioning from a mineral-dominated system to a more organic-rich system. The orgMAR and MDR for the freshwater and brackish marshes are presented in Figures 6 and 7, respectively, along with the temporal changes in the fraction of organic matter.

DISCUSSION

Historic Controls on Freshwater Marsh Accretion

The freshwater marshes have a predominantly inorganic depositional history, best explained by proximity (100–200 m) of each site to the Mobile and Tensaw River channels. This observation appears to be consistent with other freshwater marshes within the southeastern U.S.A. (Neubauer, 2008). Based on a compilation of 76 tidal freshwater marshes throughout the Gulf of Mexico and Atlantic coast, inorganic sedimentation was quantitatively more important to the vertical accretion of marsh

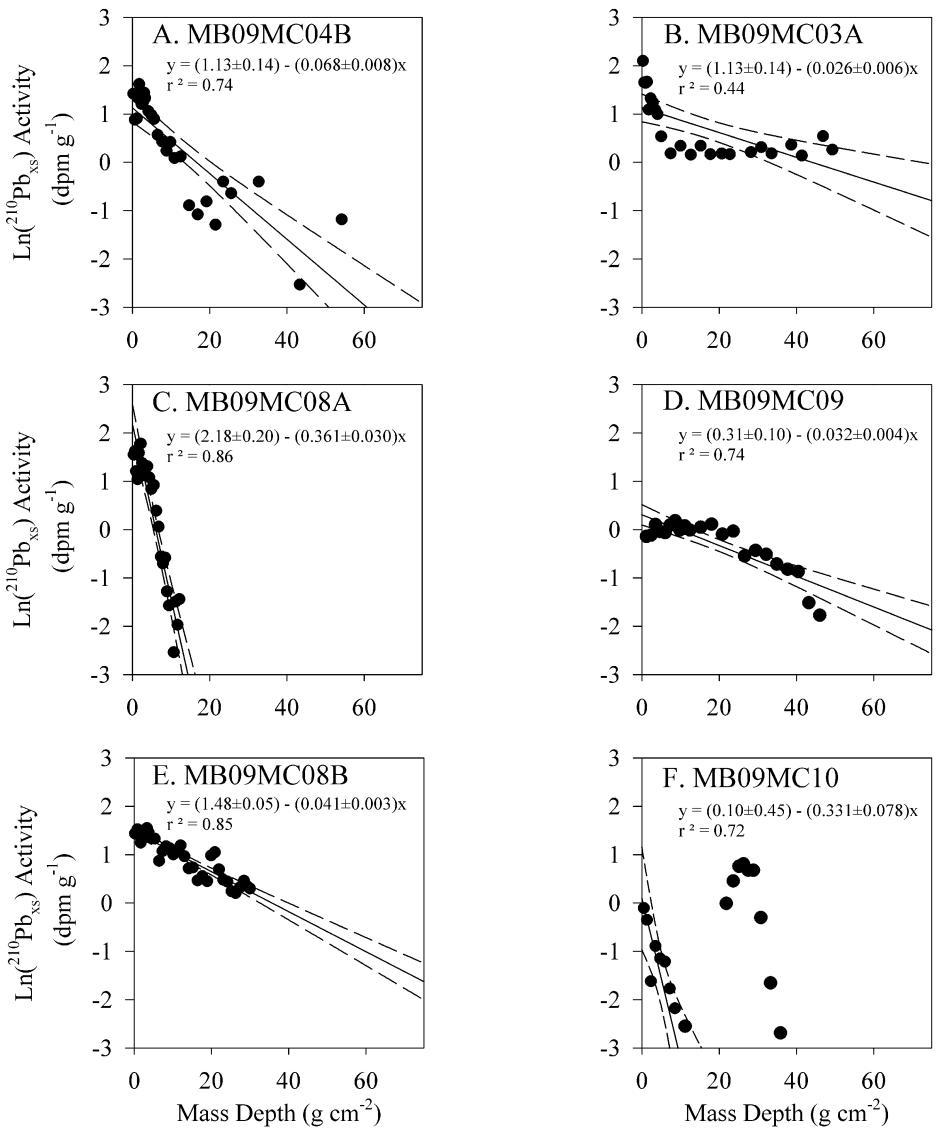

Figure 3. (Panels A–F) Plots of the natural log transform of $^{210}Pb_{xs}$ versus mass depth used to extract mass accumulation rates for each marsh core following the constant flux-constant supply model. Linear regression parameters (±error) and regression coefficients are provided for reference. A summary of the mass accumulation rates is provided in Table 2.

types than vertical organic matter accumulation (Neubauer, 2008). Tidal freshwater marshes are subject to both tidal exchange and riverine inputs. Overbank flow from the river focuses inorganic sediments into these environments (Mitsch and Gosselink, 2000; Orson, Simpson, and Good, 1990), while tidal currents flush the pore waters with oxygen and deliver nutrients to the plants (Delaune, Smith, and Sarafyan, 1986; Morse, Megonigal, and Walbridge, 2004; Orson, Simpson, and Good, 1992). Both freshwater marsh cores from the Mobile Bay-head Delta support this generalization of sediment provenance; however, there is a notable increase in organic matter accumulation over the last 40–50 years.

The initial increase in orgMARs follows closely a period of higher than average MARs (Figure 6). Closer inspection of the temporal variation in organic matter content and accumulation rates show that the increase in orgMARs is from high MARs and not f_{OM}. In fact, the organic matter content decreases slightly during this period, suggesting that the increase in MAR was in part due to changes in the abundance of inorganic sediment delivered to the freshwater marshes. Stream discharge measured along Chickasaw Creek (U.S. Geological Survey (USGS) Gage Station 02471001; USGS, 2012) show several high-flow events that occurred between 1951 (year gage installed) and early to mid-1960s (Figure 6). In fact, four of the ten highest peak flows

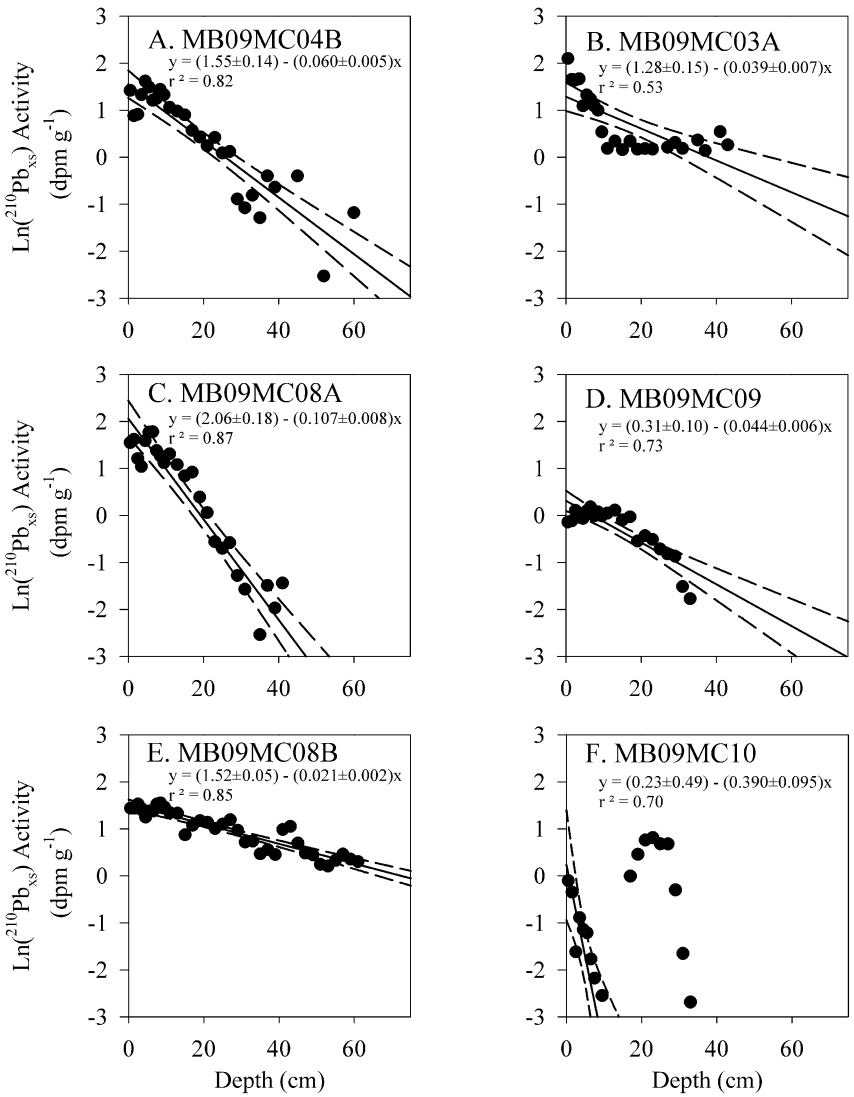

Figure 4. (Panels A–F) Plots of the natural log transform of $^{210}Pb_{xs}$ versus linear depth used to extract linear sedimentation rates (*i.e.*, marsh accretion) for each marsh core following the constant flux-constant supply model. Linear regression parameters (±error) and regression coefficients are provided for reference. A summary of the mass accumulation rates is provided in Table 2.

were measured in the 15-year period between 1950–1965 with the highest (1955) associated extensive flood event.

Commensurate with the period of high MAR and high episodic stream discharge was the construction of new lock and dams systems upstream along the Tombigbee River followed by widening of the river channel. A common problem associated with lock and dam construction is sedimentation at the reservoir site and loss of sediment load downstream. Blum and Roberts (2009) showed that decreased sediment loads along the Mississippi River were largely due to lock and dam construction during the early 1900s and were starving coastal Louisiana marshes of inorganic sediments. Along the Tombigbee–Alabama and Tensaw–Mobile Rivers, five lock and dam structures were constructed between 1937 and 1966 to replace 17 aging smaller

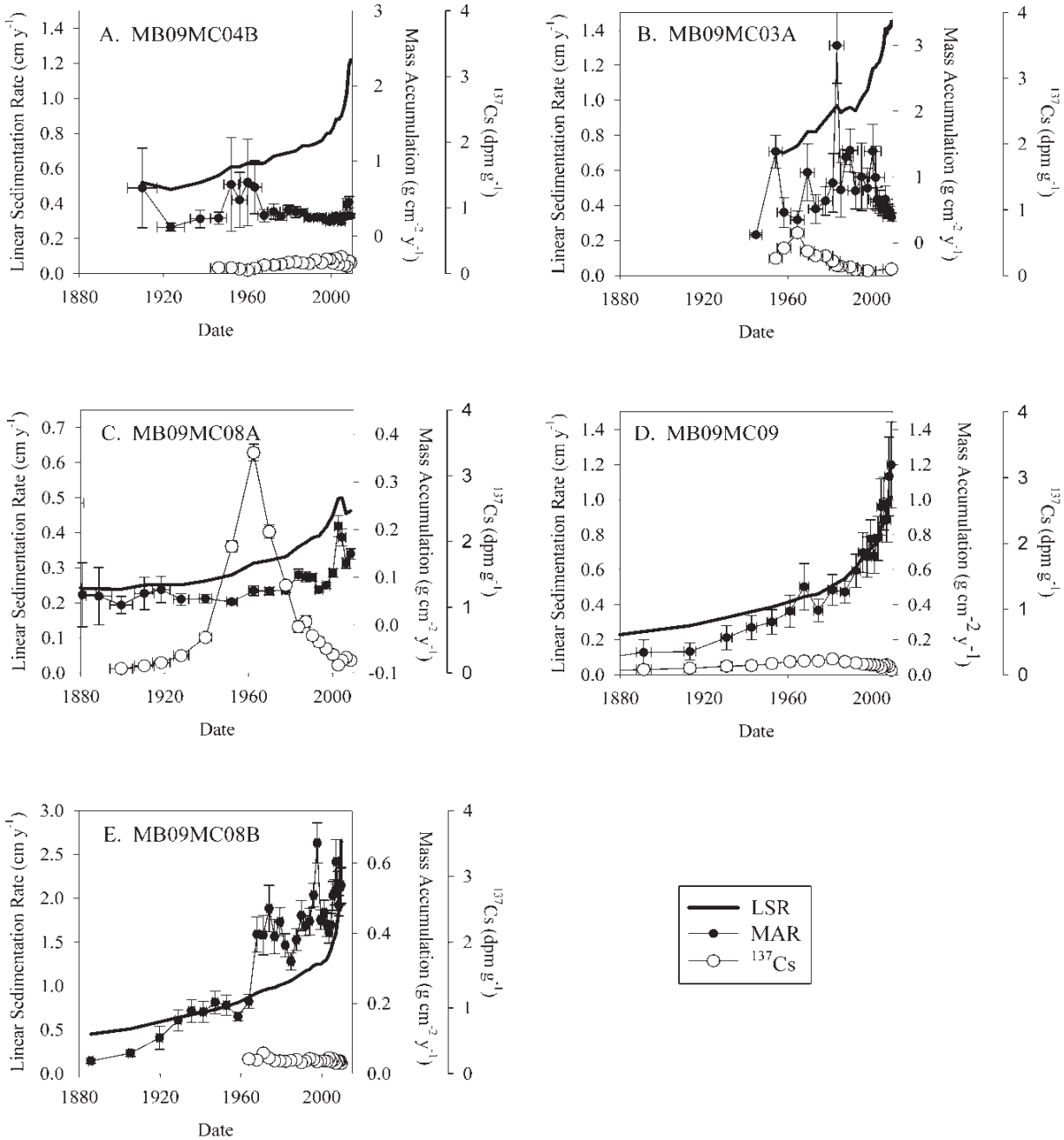

Figure 5. (Panel A–E) Time-series plots of linear sedimentation rates, mass accumulation rates, and the cesium-137 (^{137}Cs) concentrations. The temporal distribution of ^{137}Cs is used to validate the age-depth relationship represented by the abscissa. MB09MC10 is not shown because the fragmented ^{210}Pb profile resulted in unreliable CRS model results.

systems (Bankhead, Simon, and Klimetz, 2008). In addition to the lock and dam construction, the U.S. Army Corps of Engineers (USACE) also increased the channel width by 60 m. Unfortunately, sediment discharge records on the Tombigee–Alabama and Mobile–Tensaw River systems are incomplete to absent and thus direct comparison between sediment loads and orgMAR or MDR is not possible. However, based on the depositional history preserved in the marsh, discharge data, and historical account of dam construction, we hypothesize that the increase in MARs correspond to higher flows observed in the stream gage records and may even reflect enhanced sediment fluxes due to the abandonment or destruction of the older lock and dam systems. The completion of the new lock and dam systems subsequently reduced inorganic sediment loads between 1950 and 1960, thereby increasing the importance of organic accumulation in these marshes.

Inorganic Sedimentation in Brackish Marshes

Collectively, the Mobile Bay brackish marsh study sites indicate that the importance of inorganic sediment supply to the marsh accretion may be geographically different (Figure 7). For example, organic accumulation is historically much more important for the western marsh site (MC08A) than for the eastern marsh site (MC09), despite similarities in geomorphic setting (interior) and plant community (*Juncus romerianus*). The same observation holds for the fringing marsh sites; the average organic matter content (12%) accumulated in the western marsh over the last 120 years is more than twice that of the eastern fringing marsh (5.2%). Such observations reflect a potential difference in sediment source, the overall energy input into the environment, or both.

The importance of inorganic sedimentation decreases from fringing or shoreline marshes to more interior isolated marshes (Oertel, Wong, and Conway, 1989). Tidal exchange, eolian processes, and storm flooding provide local inorganic sediment sources to coastal marshes stored in tidal rivers and creeks, the adjacent estuary, or the subaerial nearshore (Oertel, Wong, and Conway, 1989; Reed, 1990; Stumpf, 1983; Turner, Swenson, and Milan, 2002). The magnitude of sediment flux decreases exponentially as the distance from the source increases (French, 2006). The overall abundance (90–96%) of inorganic sediment in the eastern marsh (MC09) suggests a proximal sediment source (Figure 7B). A detailed investigation of the bay-bottom sediments by Isphording and Lamb (1979) showed that sediments along the eastern portion of Bon Secour Bay (near MC09) were generally fine to silty sand, and form extensive (sandy) strandplain beaches with sparse vegetation (Isphording, 1983; Isphording and Lamb, 1979). The persistence of inorganic sediment at this marsh site through the 20th century suggests continuous inorganic sediment

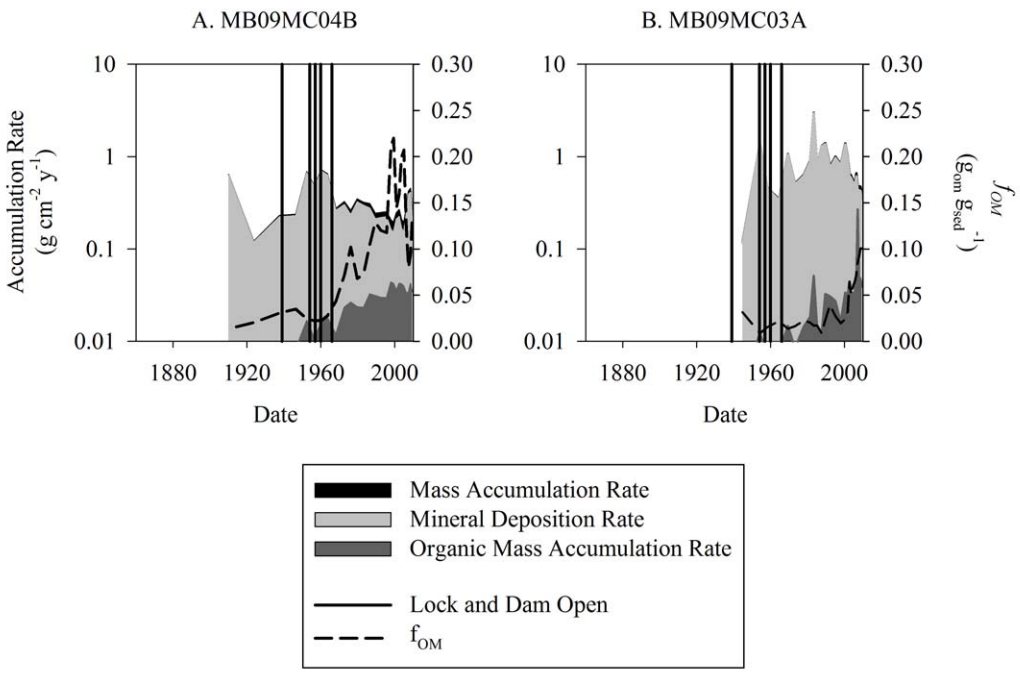

Figure 6. Time-series plot of mass accumulation rates (MARs), mineral deposition rates (MDRs), and organic mass accumulation rates (orgMARs) for the two tidal freshwater marshes (MB09MC04B–Panel A and MB09MC03A–Panel B) collected from the Mobile–Tensaw River Bayhead Delta. The precision of the ^{210}Pb ages ranges between 2% (younger sediments) and 8% (older sediments). Fraction of organic matter (f_{OM}) is presented to highlight the inverse relationship between MAR and f_{OM} observed in both cores. The completion of the five new lock and dam navigational structures closely corresponds to the initiation of organic matter (OM) accumulation and gradual increase in importance of OM accumulation to marsh accretion. MB09MC10 is not shown because the fragmented ^{210}Pb profile resulted in unreliable CRS model results.

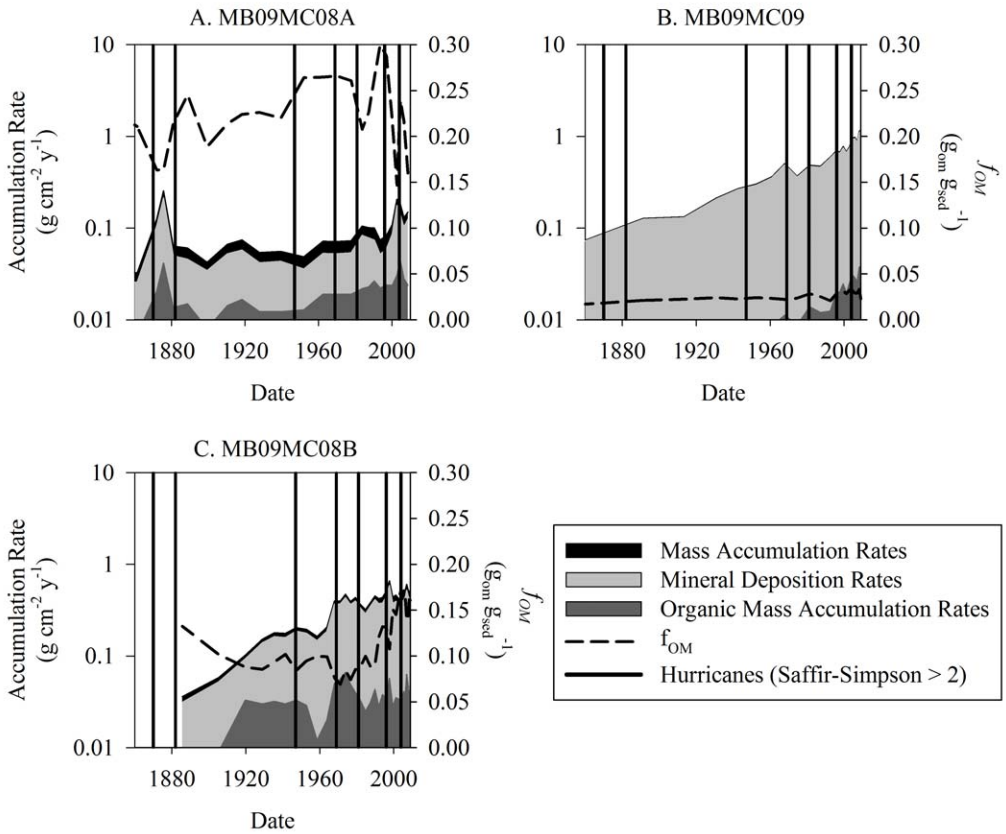

Figure 7. Time-series plot of mass accumulation rates (MARs), mineral deposition rates (MDRs), and organic mass accumulation rates (orgMARs) for three of the four brackish marsh sites (MB09MC08A–Panel A; MB09MC09–Panel B; MB09MC08B–Panel C). Fraction of organic matter (f_{OM}) is presented to highlight the inverse relationship between MAR and f_{OM} observed in several cores and subsequently used to identify possible event layers. Historically documented hurricanes with a magnitude of 2+ on the Saffir-Simpson scale are also presented on the same temporal-scale. Considering that the precision of the ^{210}Pb ages range between 2% (younger sediments) and 8% (older sediments), there is relatively good agreement between the event layers and historic hurricanes. MB09MC10 is not shown because the fragmented ^{210}Pb profile resulted in unreliable CRS model results.

flux from tidal exchange or eolian transport, or both, rather than episodic deposition.

In contrast, MAR for the two marsh sites on the west side of the bay show relatively stable marsh accretion over the last 60–120 years (Figure 7A). In MC08A, the nearly constant ratio of organic and inorganic sediments through the entire record indicates an accreting marsh surface equilibrated to inorganic sedimentation (Andersen, Svinth, and Pejrup, 2011). Similarly, the fringing marsh (MC08B) has had fairly constant MAR for the last 50 years with fairly stable inorganic sedimentation and organic accumulation. Prior to the 1960s, the accretion at this site accelerated from the late 1800s to the 1920s and orgMAR increased.

Low organic matter, high bulk density sediment layers fragment both marsh core sedimentary records and enhance MARs. Similar stratigraphic sequences observed in lake sediments (Liu

Table 3. *A list of proposed event layers (depth and time) observed in the marsh cores and hurricanes (name, magnitude, and year) that occurred during the proposed event window.*

Proposed Event Layer	Core Observed	Depth (cm)	Corresponding Hurricane Name	Saffir-Simpson Scale	Year
1867–1887	MB09MC08A	33	Mobile, Unnamed	2, 1	1870, 1882
1941–1951	MB09MC08B	41	Unnamed	3	1947
1967–1971	MB09MC08A, B	13, 39	Camile	5	1969
1977–1982	MB09MC08A	9.5	Fredric	3	1979
1997–2001	MB09MC08A, B	2.5, 7.5	Georges	4	1998
2004	MB09MC08A, B	0.5, 2.5	Ivan	3	2004

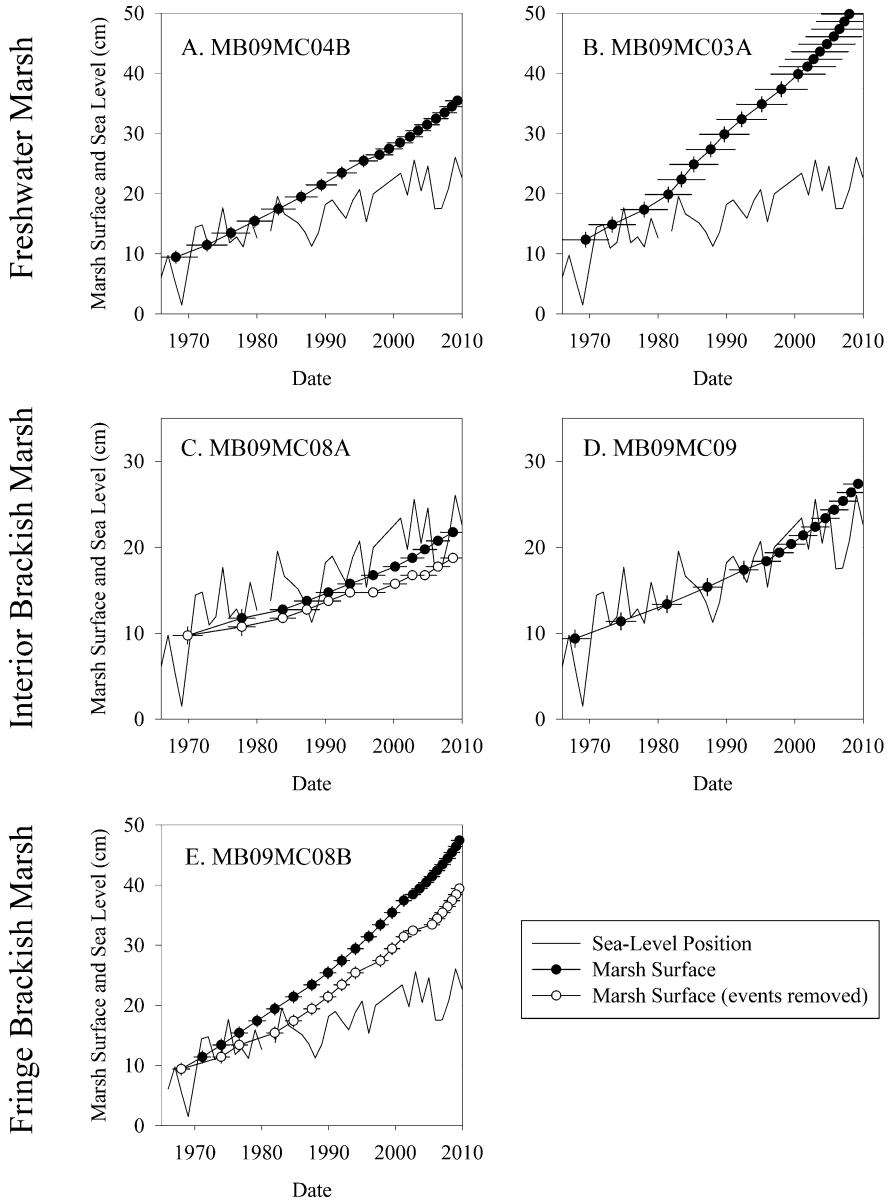

Figure 8. A plot showing temporal changes in the extrapolated marsh surface for each site (assuming uniform compaction throughout the core of the magnitude as indicated in Table 1) and annual sea level position (Dauphin Island Tidal Station, NOAA, 8735180, http://tidesandcurrents.noaa.gov/sltrends/sltrends_station.shtml?stnid=8735180 Dauphin Island, Alabama). Notably, all the marsh surfaces are keeping pace with recent sea-level rise; however, the importance of event related deposition to the marsh surfaces is highlighted in MB09MC08A and MB09MC08B (Panels C and F). Removal of a 1-cm thick event layer for the three post 1970 events reduces the marsh surface of MB09MC08A to lower than sea level, showing the vulnerability of some these marshes to rapid sea-level rise and also the importance of inorganic deposition.

and Fearn, 1993, 2000) and marsh environments (de Groot, Veeneklaas, and Bakker, 2011; Oertel, Wong, and Conway, 1989; Turner *et al.*, 2006, 2007; Turner, Swenson, and Milan, 2002) have been attributed to tropical cyclones. Recognizing that these lithologically distinct layers represent deviations from average hydrodynamic forces affecting the marsh (Bellucci *et al.*, 2007; de Groot, Veeneklaas, and Bakker, 2011), we infer that tropical cyclones are the most likely candidate for moving inorganic sediments stored in the bay to the marsh surface. In the top 7–10 cm (*i.e.*, <12 yr B.P.) of both western marsh cores, two well-preserved layers temporally coincide with the passage of Hurricane Georges in 1998 and Hurricane Ivan in 2004. While Hurricane Georges did not directly hit the Mobile Bay region, the surge observed at Fort Morgan and into the bay

was on the order of 3–4 m causing considerable coastal flooding (Blake, Landsea, and Gibney, 2011). Hurricane Ivan caused considerable damage and erosion to the Gulf as the hurricane made two landfalls, the first being just east of Mobile Bay. Surge in the bay was typically less than 2 m; however, higher than prestorm water levels resonated within the bay for more than 48 hours (Park *et al.*, 2007).

For both Hurricane Georges and Hurricane Ivan, the f_{OM} in the two layers (1-cm thick) decreased by greater than or equal to 5% relative to adjacent (pre and post) layers. Similarly, the MARs increased by as much as 25% above the long-term mean during emplacement of the two event layers. Using the relative changes in f_{OM} and MAR during the two near modern events as guides, we identify four additional events preserved in the marsh record at the western marsh sites (Table 3). According to the report by Blake, Landsea, and Gibney (2011) and our core record, all six suspected event layers bracket periods when major hurricanes (Saffir-Simpson scale >2) passed within 100 km of the bay. Beyond our two models, the most discernible event layer corresponds to Hurricane Fredric (1979), which has been characterized as the most intense storm to affect the Mobile Bay region during the 1900s (Isphording and Imsand, 1991). Estimates of bathymetric change (0.35 m increase in depth) and suspended sediment loads (six times greater than the daily average) provide the best analogy of sediment remobilization during Hurricane Fredric (Isphording and Imsand, 1991). Storm surge in the Gulf of Mexico overwashed the Morgan Peninsula transporting sand inland and depositing it as storm-event layers in Lake Shelby, Alabama (U.S.A.) (Liu and Fearn, 1993). With such intensity, the effects of Hurricane Fredric should have been evidenced bay wide, and based on the other brackish cores, it probably was.

The records of ^{210}Pb and ^{137}Cs are not well preserved in MC10 and thus the geochronology is poorly constrained relative to the other cores (Figure 2). However, the activity of ^{137}Cs at 23 cmbls and below the large event layer in this core is comparable to the activities observed during the middle to late 1960s in MC08A. Based on this analogy, the deposition of the event layer took place sometime after the 1960s. The relative ages bracket the layer as a potential deposit associated with Hurricane Camille, Hurricane Fredric, or more realistically, both. Unlike the marsh sites along the western shoreline, the thickness of the event layer at this site exceeded 8 cm. The difference in the volume of sediment added to the marsh surface again reflects the sediment availability and the overall flooding depth. Based on the slow gradual increase in OM, it has taken the marsh almost 20 years to return to prestorm productivity.

Marsh Response to Sea-Level Rise

Marsh accretion observed in the subset of marshes sampled for this study is very different from one geographic region to another. Linear sedimentation rates vary by almost a full order of magnitude. However, for every marsh site assessed, modern LSRs exceed the average local relative sea-level rise (RSLR) of approximately 0.3 cm y^{-1} observed at Dauphin Island Marine Lab (NOAA, 2012; Figure 8). Historically, the availability of inorganic sediment supply to the tidal freshwater marshes has helped maintain a stable marsh surface relative to the accelerated sea-level rise. The current trend observed in both freshwater marsh cores (*i.e.*, increase in orgMAR) does not appear to be affecting the marshes' ability to keep pace with relative sea-level rise. As with the Louisiana marshes, decreases in stream load sediments due to lock and dam construction will have a negative impact on emergent wetlands that are dependent on inorganic sedimentation.

In marshes examined as part of this study, the brackish marshes are the most susceptible to a rise in sea level, whether occurring at a rapid pace or gradually through time. The marsh sites assessed around Mobile Bay have and continue to fare well with respect to sea-level changes. At all four marsh sites, accretion rates were comparable or greater than local RSLR (Table 2); however, the previous discussion on inorganic sediment fluxes highlights an important question for these coastal marshes when considering sea-level rise: What role does inorganic sediment supply play in maintaining the marsh elevation relative to sea level? This question has been a topic of much discussion for marshes in Louisiana and around the world. For example, Nyman, Crozier, and Delaune (1995) argued that the volume of inorganic sediment delivered inland during Hurricane Andrew (1992) benefited the coastal marshes, providing nutrients, substrate, and elevation for these rapidly subsiding wetlands. Wetland accretion increased by over 400% relative to the 30-year average due to this one event (Nyman, Crozier, and Delaune, 1995). Turner *et al*. (2006) showed similar large sediment fluxes to Louisiana coastal wetlands following Hurricanes Katrina and Rita; however, the contribution to net marsh accretion has been debated (Burkett, Groat, and Reed, 2007; Törnqvist *et al.*, 2007). For the salt marshes along the Netherlands and Denmark coastlines, sand supplied by high-energy events constitutes a major component of marsh accretion (de Groot, Veeneklaas, and Bakker, 2011).

From the historic mineral deposition rates within the various cores examined, it is apparent that Mobile Bay marshes are not as sediment starved as marshes in other areas of the Gulf of Mexico coast. In general, the importance of event-related, inorganic sedimentation to marsh accretion will be most important where physiochemical conditions (*e.g.*, porewater salinity, oxidation-reduction potential, and flood frequency) retard vegetative growth and organic accumulation. MC08A represents the only marsh that we can comfortably argue may be threatened by sea-level rise. Based on the organic matter content, approximately 30–50% of its vertical accretion is reliant on organic accumulation while the remaining 50–70% is inorganic sedimentation. To evaluate the contribution of event-layer sedimentation on the long-term accretion of the marsh, we modified the depositional history of the marsh associated with core MC08A by extracting all of the proposed event layers (1 cm each) and recomputing the marsh surface through time (Figure 8C). Based on the model, marsh accretion was able to keep pace with the modern sea-level position until the 1990s, when a slight increase in the rate of SLR occurred relative to the previous 20 years. Overall, marsh accretion based on the eventless model (0.23 cm y^{-1}) is approximately 20% less than the long-term average with event sedimentation. Without inorganic sedimentation due to Hurricanes Georges and Ivan, the marsh may have reverted to open water.

CONCLUSION

This study examined marsh accretion and sedimentation in the Mobile Bay and bayhead delta region. Coastal marshes largely depend on a dynamic balance between inorganic sedimentation and organic matter accumulation in order to vertically accrete. Marshes in this region have historically been and continue to be dependent largely on inorganic sedimentation to maintain the marsh surface above mean sea level. The proximity of freshwater marshes to the Mobile–Tensaw Rivers, with their large sediment loads, has provided a continual source of sediment to these marshes. However, anthropogenic modifications for navigation and flow control along the rivers may be decreasing this sediment source and contributing to the observed shift to more dependence on organic matter accumulation. Brackish marshes in the lower part of the bay show a similar reliance on inorganic sedimentation. Three of the four marshes had inorganic sedimentation rates that were greater than 90% of the net mass accumulation. In marshes with higher organic matter accumulation, mineral deposition often occurred episodically in response to major hurricanes or tropical cyclones.

ACKNOWLEDGEMENTS

Funding for this research was provided by the USGS Coastal and Marine Geology Program as part of the Northern Gulf of Mexico Ecosystem Change and Hazard Susceptibility Project. The authors would like to thank Christopher Reich, Adis Muslic, Jeffrey Frazier, Margaret Marot, and Katie Richwine of the USGS for their continued support in the lab and in the field, and Dr. Joseph Smoak and Thomas Harmon (University of South Florida–St. Petersburg). Any use of trade names is for descriptive purposes only and does not represent endorsement by the U.S. Geological Survey or the Federal Government.

LITERATURE CITED

Andersen, T.J.; Svinth, S., and Pejrup, M., 2011. Temporal variation of accumulation rates on a natural salt marsh in the 20th century: The impact of sea-level rise and increased inundation frequency. *Marine Geology,* 279, 178–187.

Appleby, P.G., 2001. Chronostratigraphic techniques in recent sediments. *In:* Last, W.M. and Smol, J.P. (eds.) *Tracking Environmental Change Using Lake Sediments.* Netherlands: Springer, pp. 171–203.

Appleby, P.G. and Oldfield, F., 1978. The calculation of lead-210 dates assuming a constant rate of supply of unsupported ^{210}Pb to the sediment. *CATENA,* 5, 1–8.

Appleby, P.G. and Oldfield, F., 1992. Application of lead-210 to sedimentation studies. *In*: Ivanovich, M. and Harman, R.S. (eds.), *Uranium-Series Disequilibrium: Application to Earth, Marine, and Environmental Sciences.* Oxford: Clarendon Press, pp. 731–778.

Bankhead, N.B.; Simon, A., and Klimetz, D., 2008. Analysis of Streambank Erosion Along the Lower Tombigbee River, Alabama. U.S. Department of Agriculture–Agricultural Research Service. *National Sedimentation Laboratory Research Report No. 62*, 82p.

Baskaran, M., 2011. Po-210 and Pb-210 as atmospheric tracers and global atmospheric Pb-210 fallout: A review. *Journal of Environmental Radioactivity*, 102(5), 500–513.

Bellucci, L.G.; Frignani, M.; Cochran, J.K.; Albertazzi, S.; Zaggia, L.; Cecconi, G., and Hopkins, H., 2007. Pb-210 and Cs-137 as chronometers for salt marsh accretion in the Venice Lagoon-Links to flooding frequency and climate change. *Journal of Environmental Radioactivity,* 97(2-3), 85–102.

Binford, M.W., 1990. Calculation and uncertainty analysis of ^{210}Pb dates for PIRLA project lake sediment cores. *Journal of Paleolimnology,* 3, 253–267.

Blake, E.S.; Landsea, C.W., and Gibney, E.J., 2011. The Deadliest, Costliest, and Most Intense United States Tropical Cyclones from 1851 to 2010 (and Other Frequently Requested Hurricane Facts*). NOAA Technical Memorandum NWS NHC-6*, 47p.

Blum, M.D. and Roberts, H.H., 2009. Drowning of the Mississippi Delta due to insufficient sediment supply and global sea-level rise. *Nature Geoscience*, 2, 488–491.

Breitzke, M., 2006. Physical properties of marine sediments. *In:* Schulz, H.D. and Zabel, M. (eds.), *Marine Geochemistry.* Berlin: Springer, pp. 27–71.

Burkett, V.; Groat, C.G., and Reed, D., 2007. Hurricanes not the key to a sustainable coast. *Science,* 315, 1366–1368.

Childers, D.L. and Day, J.W., 1990. Marsh-water column interactions in two Louisiana estuaries, I. Sediment dynamics. *Estuaries,* 13(4), 393–403.

Curtis, W.F.; Culbertson, J.J., and Chase, E.B., 1973. Fluvial-Sediment Discharge to the Oceans from the Conterminous United States. *U.S. Geological Survey Circular 670,* 17p.

Cutshall, N.H.; Larsen, I.L., and Olsen, C.R., 1983. Direct analysis of ^{210}Pb in sediment samples: Self-absorption corrections. *Nuclear Instruments and Methods B,* 206, 309–312.

De Groot, A.V.; Veeneklaas, R.M., and Bakker, J.P., 2011. Sand in the salt marsh: Contribution of high-energy conditions to salt-marsh accretion. *Marine Geology,* 282, 240–254.

DeLaune, R.D.; Smith, C.J., and Sarafyan, M.N., 1986. Nitrogen cycling in a freshwater marsh of *Panicum Hemitomon* on the deltaic plain of the Mississippi River. *Journal of Ecology,* 74, 249–256.

Flessa, K.W.; Constantine, K.J., and Cushman, M.K., 1977. Sedimentation rates in coastal marshes determined from historical records. *Chesapeake Science,* 18, 172–176.

French, J., 2006. Tidal marsh sedimentation and resilience to environmental change: Exploratory modelling of tidal, sea level and sediment supply forcing in predominantly allochthonous systems. *Marine Geology,* 235, 119–136.

Harrison, E.Z. and Bloom, A.L., 1977. Sedimentation rates on tidal salt marshes in Connecticut. *Journal of Sedimentary Research,* 47, 1484–1490.

IPCC, 2007. *Climate Change 2007: Impacts, Adaptation and Vulnerability. Contribution of Working Group II to the Fourth Assessment Report of the Intergovernmental Panel on Climate Change.* United Kingdom and New York: Cambridge University Press, 976 p.

Isphording, W.C., 1983. Chemistry and partitioning of heavy metals in Mobile Bay, Alabama. *In:* Tanner, W. F. (ed.), *Near-Shore Sedimentology: Proceedings from the 6th Symposium on Coastal Sedimentology* (Tallahassee, Florida), pp. 184–200.

Isphording, W.C. and Imsand, F.D., 1991. Cyclonic events and sedimentation in the Gulf of Mexico. *Coastal Sediments 1991,* (Seattle, Washington), pp. 1122–1136.

Isphording, W.C. and Lamb, G.M., 1979. The Sediments of Mobile Bay. *Dauphin Island Sea Lab Report 80-002,* 31p.

Kindinger, J.L.; Balson, P.S., and Flocks, J.G., 1994. Stratigraphy of the Mississippi–Alabama shelf and the Mobile River incised-valley system. *In:* Dalrymple, R.W.; Boyd, R., and Zaitlain, B.A. (eds.), *Incised-Valley Systems: Origin and Sedimentary Sequences.* Tulsa, Oklahoma: Society for Sedimentary Geology, pp. 83–95.

Kirwan, M.L. and Murray, A.B., 2007. A coupled geomorphic and ecological model of tidal marsh evolution. *Proceedings of the National Academy of Sciences,* 104, 6118–6122.

Kirwan, M.L. and Murray, A.B., 2008. Tidal marshes as disequilibrium landscapes? Lags between morphology and Holocene sea-level change. *Geophysical Research Letters,* 35, L24401.

Kolker, A.S.; Goodbred, S.L., Jr.; Hameed, S., and Cochran, J.K., 2009. High-resolution records of the response of coastal wetland systems to long-term and short-term sea-level variability. *Estuarine, Coastal and Shelf Science,* 84, 493–508.

Liu, K.B. and Fearn, M.L., 1993. Lake-sediment record of Late Holocene hurricane activities from coastal Alabama. *Geology,* 21, 793–796.

Liu, K.B. and Fearn, M.L., 2000. Reconstruction of prehistoric landfall frequencies of catastrophic hurricanes in northwestern Florida from lake sediment records. *Quaternary Research,* 54, 238–245.

Mars, J.C.; Shultz, A.W., and Schroeder, W.W., 1992. Stratigraphy and Holocene evolution of Mobile Bay in southwestern Alabama. *Gulf Coast Association of Geological Societies,* 42, 529–542.

May, E.B., 1976. Holocene sediments of Mobile Bay, Alabama. *In:* Swingle, H.G.; Powell, M.R.; Swingle, W.E., and Tatum, W.M. (eds.) *Alabama Marine Resources Bulletin, No. 11,* pp. 1–25.

Milan, C.S.; Swenson, E.M.; Turner, R.E., and Lee, J.M., 1995. Assessment of the ^{137}Cs method for estimating sediment accumulation rates: Louisiana salt marshes. *Journal of Coastal Research,* 11, 296–307.

Mitsch, W.J. and Gosselink, J.G., 2000. *Wetlands,* New York: Wiley, 920p.

Moorhead, K.K. and Brinson, M.M., 1995. Response of wetlands to rising sea level in the lower coastal plain of North Carolina. *Ecological Applications,* 5, 261–271.

Morris, J.T.; Sundareshwar, P.V.; Nietch, C.T., Kjerfve, B., and Cahoon, D.R., 2002. Responses of coastal wetlands to rising sea level. *Ecology,* 83, 2869–2877.

Morse, J.L.; Megonigal, J.P., and Walbridge, M.R., 2004. Sediment nutrient accumulation and nutrient availability in two tidal freshwater marshes along the Mattaponi River, Virginia, U.S.A. *Biogeochemistry,* 69, 175–206.

Neubauer, S.C., 2008. Contributions of mineral and organic components to tidal freshwater marsh accretion. *Estuarine Coastal and Shelf Science,* 78, 78–88.

NOAA, 2012. Mean sea-level trend 8735180 Dauphin Island, Alabama. Silver Spring, Maryland: National Oceanic and Atmospheric Administration, *NOS Tides and Currents*. URL: http://tidesandcurrents.noaa.gov/sltrends/sltrends_station.shtml?stnid=8735180 Dauphin Island, Alabama; accessed on June 7, 2011.

Nyman, J.A.; Crozier, C.R., and Delaune, R.D., 1995. Roles and patterns of hurricane sedimentation in an estuarine marsh landscape. *Estuarine Coastal and Shelf Science,* 40, 665–679.

Oertel, G.; Wong, G., and Conway, J., 1989. Sediment accumulation at a fringe marsh during transgression, Oyster, Virginia. *Estuaries and Coasts,* 12, 18–26.

Orson, R.A.; Simpson, R.L., and Good, R.E., 1990. Rates of sediment accumulation in a tidal freshwater marsh. *Journal of Sedimentary Petrology,* 60, 859–869.

Orson, R.A.; Simpson, R.L., and Good, R.E., 1992. A mechanism for the accumulation and retention of heavy metals in tidal freshwater marshes of the upper Delaware River estuary. *Estuarine Coastal and Shelf Science,* 34, 171–186.

Otvos, E.G., 2004. Holocene Gulf levels: Recognition issues and an updated sea-level curve. *Journal of Coastal Research,* 20, 680–699.

Park, K.; Valentine, J.F.; Sklenar, S.; Weis, K.R., and Dardeau, M.R., 2007. The effects of Hurricane Ivan in the inner part of Mobile Bay, Alabama. *Journal of Coastal Research,* 23, 1332–1336.

Patrick, W.H., Jr. and Delaune, R.D., 1990. Subsidence, accretion, and sea-level rise in south San Francisco Bay marshes. *Limnology and Oceanography,* 35, 1389–1395.

Preiss, N., Mélières, M.-A., Pourchet, M., 1996. A compilation of data on lead 210 concentration in surface air and fluxes at the air-surface and water-sediment interfaces. *Journal of Geophysical Research: Atmospheres*, 101(D22), 28,847–28,862.

Redfield, A.C., 1972. Development of a New England salt marsh. *Ecological Monographs,* 42, 201–237.

Reed, D.J., 1988. Sediment dynamics and deposition in a retreating coastal salt marsh. *Estuarine, Coastal and Shelf Science,* 26, 67–79.

Reed, D.J., 1990. The impact of sea-level rise on coastal salt marshes. *Progress in Physical Geography,* 14, 465–481.

Robbins, J.A. and Edgington, D.N., 1975. Determination of recent sedimentation rates in Lake Michigan using Pb-210 and Cs-137. *Geochimica et Cosmochimica Acta,* 39, 285–304.

Rodriguez, A.B. and Meyer, C.T., 2006. Sea-level variation during the Holocene deduced from the morphologic and stratigraphic evolution of Morgan Peninsula, Alabama, U.S.A. *Journal of Sedimentary Research,* 76, 257–269.

Rodriguez, A.B.; Greene, D.L.; Anderson, J.B., and Simms, A.R., 2008. Response of Mobile Bay and eastern Mississippi Sound, Alabama, to changes in sediment accommodation and accumulation. *Geological Society of America Special Papers,* 443, 13–29.

Stumpf, R.P., 1983. The process of sedimentation on the surface of a salt marsh. *Estuarine, Coastal and Shelf Science,* 17, 495–508.

Törnqvist, T.E.; Paola, C.; Parker, G.; Liu, K.B.; Mohrig, D.; Holbrook, J.M., and Twilley, R.R., 2007. Comment on "Wetland sedimentation from Hurricanes Katrina and Rita." *Science,* 316, 201.

Turner, R.E.; Baustian, J.J.; Swenson, E.M., and Spicer, J.S., 2006. Wetland sedimentation from Hurricanes Katrina and Rita. *Science,* 314, 44–452.

Turner, R.E.; Swenson, E.M., and Milan, C.S., 2002. Organic and inorganic contributions to vertical accretion in salt marsh sediments. *In:* Weinstein, M.P. and Kreeger, D.A. (eds.), *Concepts and Controversies in Tidal Marsh Ecology.* Netherlands: Kluwer, pp. 583–595.

Turner, R.E.; Swenson, E.M.; Milan, C.S., and Lee, J.M., 2007. Hurricane signals in salt marsh sediments: Inorganic sources and soil volume. *Limnology and Oceanography,* 52, 1231–1238.

USGS, 2012. USGS Surface-water daily data for the Nation. U.S. Geological Survey. URL: http://waterdata.usgs.gov/nwis/dv/?site_no=02471001&agency_cd=USGS&referred_module=sw; accessed on June 10, 2011.